ELSEVIER

Nuclear Instruments and Methods in Physics Research A 493 (2002) 30–44

NUCLEAR INSTRUMENTS & METHODS IN PHYSICS RESEARCH Section A

www.elsevier.com/locate/nima

The silicon multiplicity detector for the NA50 experiment at CERN

B. Alessandro[a], S. Beolé[b], G. Bonazzola[b], W. Dąbrowski[c], P. Deremigis[a], P. Giubellino[a], P. Grybos[c], M. Idzik[a,c,*], A. Marzari-Chiesa[b], M. Masera[b], M. Monteno[a], W.L. Prado da Silva[d], F. Prino[e], L. Ramello[e], P. Rato Mendes[b], L. Riccati[a], M. Sitta[e]

[a] *INFN, via P. Giuria 1, 10125 Torino, Italy*
[b] *Dipartimento di Fisica Sperimentale dell'Università, Torino, Italy*
[c] *Faculty of Physics and Nuclear Techniques, University of Mining and Metallurgy, Cracow, Poland*
[d] *UERJ, Rio de Janeiro, Brazil*
[e] *DISTA, Università del Piemonte Orientale, Alessandria, Italy*

Received 10 June 2002; received in revised form 30 July 2002; accepted 31 July 2002

Abstract

The design, operation and performance of the silicon strip Multiplicity Detector for the heavy-ion experiment NA50 at CERN are presented. The main features of the detector are high speed (50 MHz sampling frequency), high granularity (more than 13,000 strips), and good radiation resistance. The detector provided a measurement of event centrality in Pb–Pb collisions, as well as target identification and the measurement of charged particle pseudorapidity distributions as a function of centrality.
© 2002 Elsevier Science B.V. All rights reserved.

PACS: 29.40

Keywords: Position sensitive detector; Silicon strip detector; Multiplicity; Heavy ion collisions; Data analysis; Experimental techniques

1. Introduction

The NA50 experiment [1] at the CERN SPS investigates the nuclear matter under extreme conditions of energy density with the ultimate goal of detecting signals of a phase transition from ordinary matter to a plasma of deconfined quarks and gluons (QGP). The NA50 experiment investigates the production of resonances decaying to dimuons in fixed-target Pb–Pb interactions at 158 A GeV/c beam momentum. In particular, the experiment is looking for dimuon production from charmonium resonances and its suppression due to Debye screening in a deconfined medium [2]. To collect enough statistics on the production of J/ψ and ψ' mesons, the experiment worked at the maximum beam intensity which was

*Corresponding author. INFN Torino, via P. Giuria 1, 10125 Torino, Italy. Tel.: +39-011-670-7372; fax: +39-011-669-9579.

E-mail address: idzik@to.infn.it (M. Idzik).

0168-9002/02/$ - see front matter © 2002 Elsevier Science B.V. All rights reserved.
PII: S0168-9002(02)01557-7

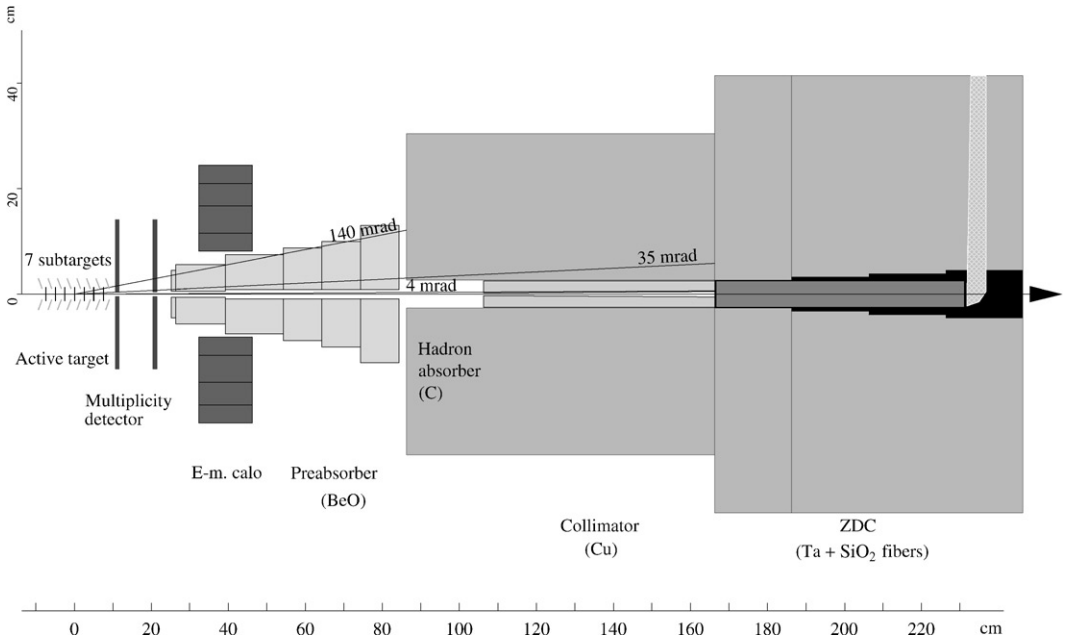

Fig. 1. Schematic view of the NA50 target region (1995–1998).

compatible with a correct operation of the various detectors, namely (1–1.4) $\times 10^7$ beam particles/s, and with a target thickness up to 32% of an interaction length. The main experimental components are: a high-resolution muon spectrometer based on toroidal magnet equipped with 4 trigger hodoscopes and 8 MWPCs, and three centrality detectors, namely a zero-degree calorimeter (ZDC) [3] for forward energy measurements, an electromagnetic calorimeter (EMC) for transverse energy measurements and a silicon microstrip Multiplicity Detector (MD) for charged multiplicity measurements. The MD can also be used for identification of the target where the interaction took place, as an alternative to the standard system based on quartz blades [4]. A segmented quartz beam hodoscope is used for the definition of the incoming beam and the detection of beam pileup, while scintillators are used to veto interactions in the beam hodoscope itself and particles in the halo of the beam. During the 1995, 1996 and 1998 runs a segmented target made of seven lead subtargets was available (in 1998 only the middle one was used), while for the 1999 and 2000 runs a new target system with a single target under vacuum was used. The overall layout of the NA50 target region is shown in Fig. 1, including targets, target identification system and the two MD planes, as well as the other centrality detectors.

2. Detectors and mechanical assembly

The MD built of silicon microstrip detectors is designed for measurement of the number and the angular distribution of charged particles produced in Pb–Pb interactions at high energy. Since the experiment takes data at very high rate, and the silicon detectors operate in the high-radiation area close to the target, the detector has to be very fast (double pulse resolution of the readout electronics <50 ns), radiation resistant (up to 20 Mrad of total ionizing dose and a fluence up to 10^{14} of equivalent 1 MeV neutrons/cm^2, as non-ionizing damage) and of high granularity. The conditions on noise, speed and radiation hardness are comparable to the ones foreseen for inner trackers [5] at the future Large Hadron Collider (LHC) at CERN.

Due to various constraints: presence of a set of seven targets distributed over 15 cm along the beam line (in order to minimize secondary interactions and photon conversions in the targets), beam width and divergence which dictate a minimum distance of the sensitive elements from the beam line, the necessary angular coverage is obtained with two identical detector planes, called MD1 and MD2, placed about 10 cm apart. The presence of two planes allows the reconstruction of "tracklets" (segments defined by one hit in MD1 and one in MD2) and consequently the use of the MD as a subtarget identification system. Each detector plane is a disc of inner radius 4.4 mm and outer radius 86.4 mm, segmented both azimuthally and radially to have almost constant occupancy per sensitive element. The microstrip detectors were designed with a segmentation in pseudorapidity (η) adapted to the expected particle density (on average, $\Delta\eta \simeq 0.02$) and with a fixed segmentation in azimuthal angle ($\Delta\phi = 10^\circ$). Each plane, MD1 and MD2, is made of two crowns, inner and outer. The main geometrical parameters of one MD plane are listed in Table 1, together with the effective pseudorapidity coverage of MD1 in 1996 and 1998, for two of the seven target positions (target position 4 was the one normally used in 1998). The effective pseudorapidity coverages include a radial outward displacement of 2.1 mm for all strips with respect to the design value, due to mechanical constraints.

Since the multiplicity detectors are exposed to high and non-uniform, radiation levels, each detector plane is built as a mosaic of silicon detectors, each assembled on an independent multilayer board together with its front-end electronics, so that they can be easily replaced in case of severe damage.

Table 1
Nominal geometrical parameters of one MD plane; effective η coverages for MD1

Det. crown	R_{in} (mm)	R_{out} (mm)	η (MD1) target 1	η (MD1) target 4	Channels per crown
1	4.4	34.4	2.4–4.0	1.9–3.5	4608
2	34.4	86.4	1.5–2.4	1.1–1.9	2304

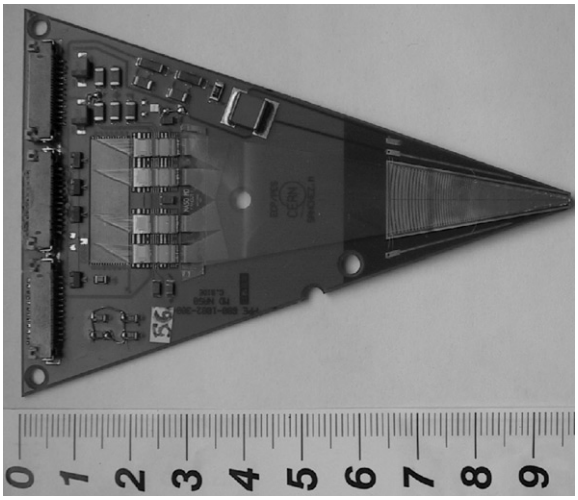

Fig. 2. BOARD1 equipped with one detector and four pairs of readout ASICs.

In particular, individual detectors[1] have either 256 strips (inner crown) or 128 strips (outer crown) and are mounted on two types of four-layer printed circuit boards called BOARD1 and, respectively, BOARD2. Detectors in the inner crown are AC-coupled to the front-end amplifier chip, while those in the outer crown are DC-coupled. Signals are brought to the front-end chips by means of 500 μm thick glass fanouts[2] with 12 μm wide A1 traces; fanouts are glued directly onto BOARD1 detectors or at the two sides of BOARD2 detectors.

Each BOARD1 is mounted onto a BOARD2 with precision pins. These pairs are then fixed on both sides of a stesalite disc, which is finally fixed to the mechanical support. Since each BOARD1 + BOARD2 pair covers a 20° azimuthal angle, 18 such pairs (9 on each side of the stesalite disc) are needed to form a full MD plane.

A large external multilayer printed circuit (EXTCARD), mechanically independent from the stesalite disc, provides electrical connections between the BOARD2s and the readout system for one detector plane. BOARD1s are connected to

[1] Detectors were fabricated by Canberra Semiconductor N.V. (now Canberra Packard Benelux), Olen, Belgium.

[2] Glass fanouts were fabricated by Optimask, Paris, France.

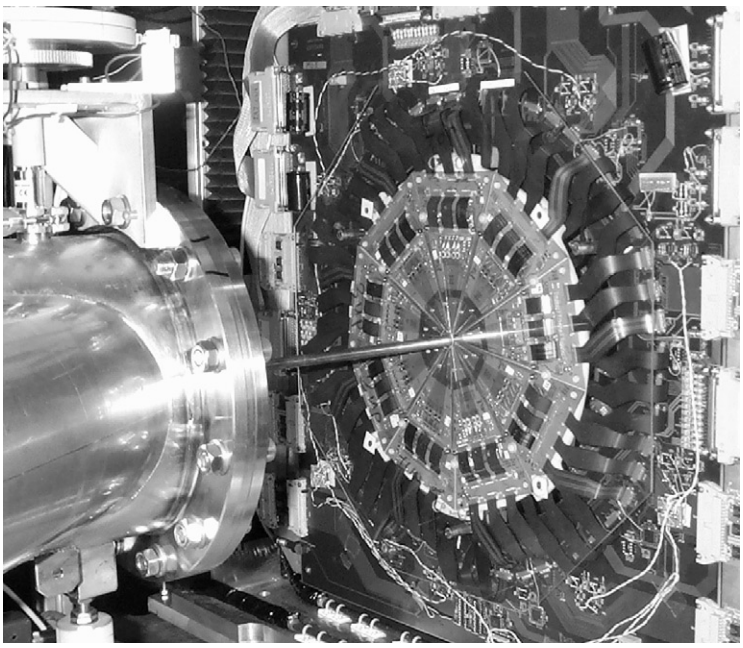

Fig. 3. Picture of MD1 during the year 2000 run (beam enters from left).

BOARD2s, and the latter to the EXTCARD, via thin and flexible kapton cables, with a pitch of 0.020″, using microflex connectors on both ends.

A photograph of the inner crown board (BOARD1), in which are visible the detector, the glass fanout and the four pairs of readout ASICs serving 256 channels in total, is shown in Fig. 2. The MD mechanical support allows remotely controlled vertical movement, in order to take the MD out of beam line during beam tuning periods. Fig. 3 shows a picture of MD1 on the beam line, together with the target under vacuum which has been retracted from the normal position.

3. The front-end electronics and readout system

In order to satisfy the experiment's requirement of a good double pulse resolution, in the multiplicity detector only the hit/no hit information from the strips is used. So a binary readout scheme has been chosen, in which the signals are immediately discriminated and only the digital information is stored in the data buffer for the trigger latency and then transmitted off-detector. The front-end electronics is based on two VLSI chips which are mounted very close to the silicon detectors. A block diagram of the MD front-end electronic chain, from the detector up to the intermediate memory called BUSIF, is shown in Fig. 4.

The first VLSI chip, FABRIC (FAst Binary Readout Integrated Circuit) [6], has been designed using a bipolar process[3] that exhibits limited sensitivity to radiation, as it has been measured [7]. Given limited drifts of parameters of the basic devices, the required radiation resistance of the chip has been achieved by proper design techniques. The FABRIC is connected to detector microstrips via the glass fanouts. It amplifies, shapes and discriminates the signals coming from 64 strips. The amplifier-shaper is designed as a bipolar cascode, closed by the feedback loop in the configuration of a transimpedance amplifier, followed by a simple gain stage with local emitter

[3] From Tektronix, Beaverton, OR, USA.

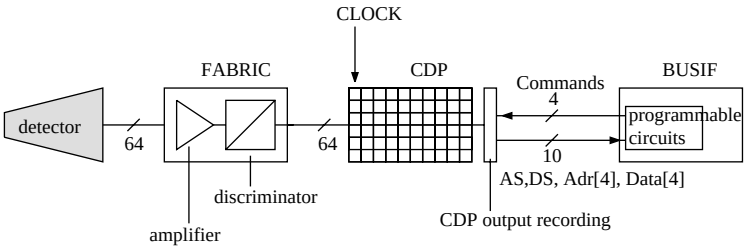

Fig. 4. Block diagram of the MD font-end electronics.

feedback and the integrator implemented in a differential pair. Its peaking time is of about 15 ns. The discriminator is designed as a simple differential comparator in the Schmitt configuration. Its walk time is less than 5 ns. The discriminator threshold is the same for all 64 channels. The double pulse resolution of the whole chip is of about 40 ns. During data taking we have actually used four independent threshold settings for different groups of FABRICs, namely for those mounted on BOARD1s (AC-coupled detectors) and BOARD2s (DC-coupled detectors), and separately on MD1 and MD2, in view of the different noise conditions for each group.

The FABRIC is directly bonded to the second chip, the Clock Driven Pipeline (CDP) [8]. CDP acts as a circular buffer working at 50 MHz frequency which stores the hit/no hit information for the trigger latency period, and then sends the data off the detector board. It is a RAM with a width of 64 rows, corresponding to the 64 output channels of the FABRIC, and with a depth of 81 columns, providing the storage of the digital information during the trigger latency (about 1 μs). The hit pattern from the FABRIC is sampled at every clock cycle and is stored into successive columns. After each trigger, the data of one column stored in CDPs are transmitted via 5 m long twisted pair cables out of the detector board. The CDP was fabricated using a radiation hard CMOS process[4].

The low voltages supplying the analog and digital chips as well as the high voltages for detector biasing are generated by commercial modules.[5] The power supplies are located in the experimental area close to the MD and the supply voltages are delivered to the EXTCARDs via 5 m long flat cables.

The readout system of MD [9] is based on three types of modules: two custom VME modules, BUS InterFace (BUSIF) and Calibration Clock and Trigger Distribution (CCTD), and the commercial B016[6] card. Each of these modules contains a transputer,[7] which is a microprocessor featuring a local memory and four high-bit-rate transmission lines (links).

The BUSIF module is used to read the data coming from CDPs and to interface the front-end electronics to the transputers of the MD acquisition system. The CCTD module generates the 50 MHz clock signal used to increment the CDP column pointer and relays to the BUSIFs the trigger signal coming from the general NA50 trigger system, aligned in phase with the clock signal, and delayed in such a way that the correct RAM column from all CDPs is read back. A TDC module measures the time interval between the NA50 trigger signal and the beginning of the clock cycle when the CDP columns are read back, in order to correct offline for possible variations of sampling efficiency.

The block diagram of the dedicated MD readout chain is shown in Fig. 5. During the trigger latency period (about 1 μs) data of a single event (a digital pattern of 64 bits × 216 CDPs) are stored in the CDPs. When the trigger signal is received, data are transmitted to the BUSIFs.

[4] From Honeywell, USA.

[5] A516 and A520 modules mounted in a SY527 crate from CAEN, Viareggio, Italy.

[6] A 16 MB dual-port memory VME module, from INMOS.

[7] Transputer models T425 and T801/T805, from INMOS.

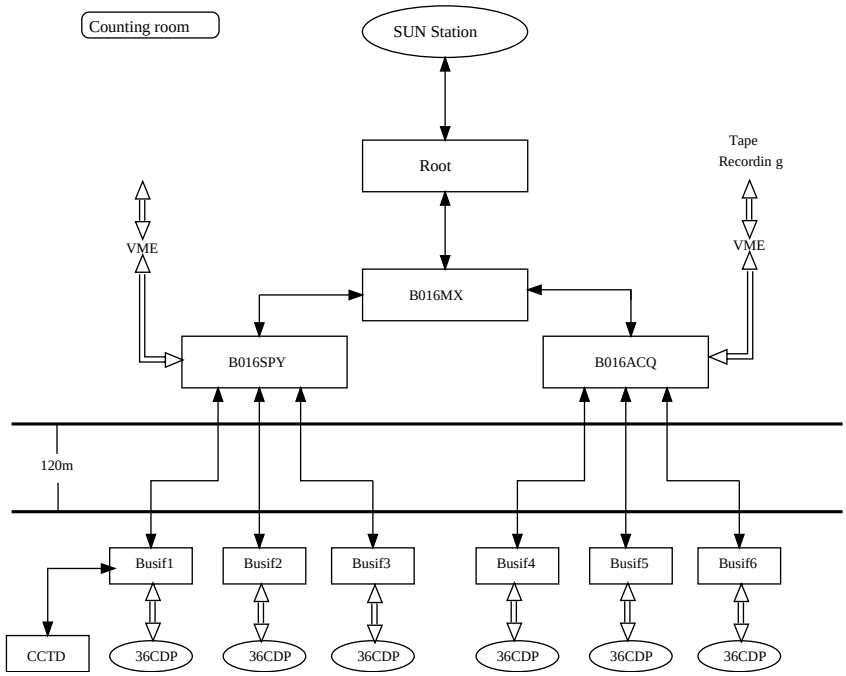

Fig. 5. Block diagram of the dedicated MD readout chain.

The data stored for the whole burst inside BUSIF modules are finally transferred to final memories in the NA50 counting room in the interburst period, during which up to 2800 events are transferred to the counting room over optical fiber transputer links (120 m long), for a total transfer time of about 7 s (the upper limit from the acquisition system is about 8–9 s). Due to instabilities found when operating the optical fiber links of the transputer network at the maximum nominal rate of 20 Mbit/s, we were forced to work at the lower rate of 10 Mbit/s, being thus limited to transfer only 2800 events per burst instead of 5000 as originally planned.

4. The monitoring system

During data taking, the MD is continuously monitored by programs that allow to check on-line the status of low and high voltages and the efficiency of individual detectors.

The monitoring of voltages is performed via a dedicated program written in C language, running under Linux RedHat 5.1 on a 486 PC. The program reads all voltages and currents from the power supply modules, performs the check against reference values and writes measured values to a log file both at regular intervals and whenever an error occurs. Groups of voltages (BOARD1 high voltages, BOARD2 high voltages, analog chip supplies and thresholds, digital chip supplies, and others) can be turned on and off together, which is important for safety reasons and for debug purposes. It is also possible to program a FABRIC discriminator threshold scan or a detector bias voltage scan.

The event monitoring program written in C/C++ language runs on a PowerPC microprocessor on the MVME 2604 card [10]. All data of BUSIFs plus the trigger, ZDC and TDC information from a whole burst are organized and written in a file so that they may be used to perform the required analysis. As an example, in Fig. 6 histograms of occupancy vs. strip number

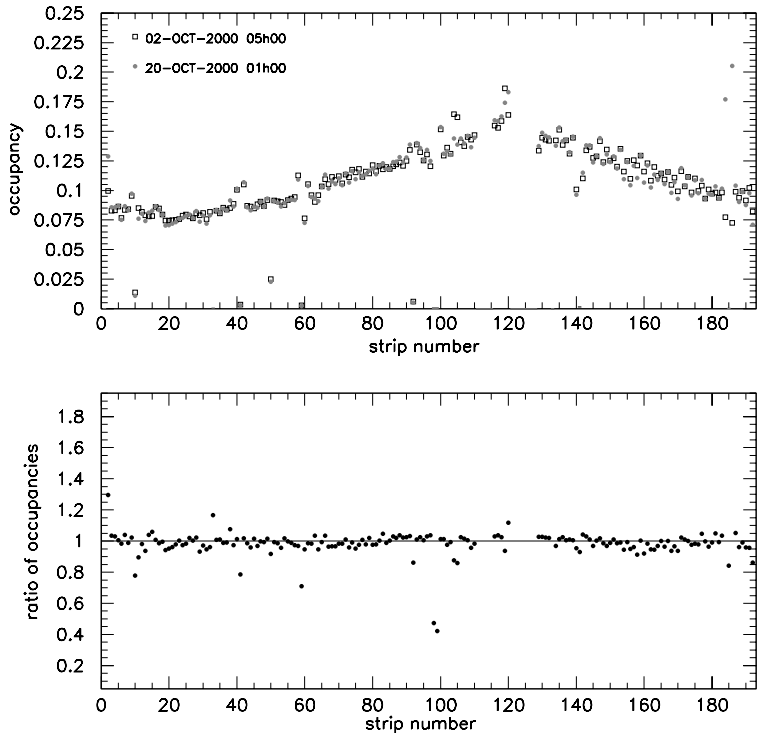

Fig. 6. Average occupancy of MD1, sector 33, for reference and current data sets (top) and the occupancy ratio between current and reference data sets (bottom).

for sector 33 of MD1 are shown. The top plot represents the occupancy from a reference data taking (beginning of year 2000 run) and from a later data taking; the bottom plot represents the occupancy ratio between the two sets (noisy channels have been masked out). This ratio was used regularly to detect any change in efficiency in every sector of MD1 and MD2.

5. Setting up of the multiplicity detector

In order to establish the initial working conditions of the MD, and to maximize the detection efficiency, it is necessary to set and periodically verify some control parameters: the trigger delay, the threshold voltage of FABRIC discriminators, and the biasing voltage of silicon detectors. This last item is strictly related to radiation damage and it is discussed in Section 6. In addition, an initial geometrical alignment on the beam line (using optical references on the mechanical support) is made at the beginning of each data taking period. Later on, the alignment is refined by using the correspondences between MD1 and MD2 strips, as described at the end of this section.

5.1. The trigger delay

The trigger latency period is about 1 μs, while the time interval necessary to have the CDP pointer on its RAM column where the triggered event is stored is 1.6 μs, corresponding to 80 clock cycles of 20 ns duration (at 50 MHz frequency). So it is necessary both to align the phase of the trigger signal with the CDP clock, and to add the right amount of delay: these two operations are performed by the CCTD module, as explained in Section 3. The optimization of the delay value is done during a series of short acquisition runs (trigger delay scan). Fig. 7 shows the results of such a scan for a typical BOARD1, both for low

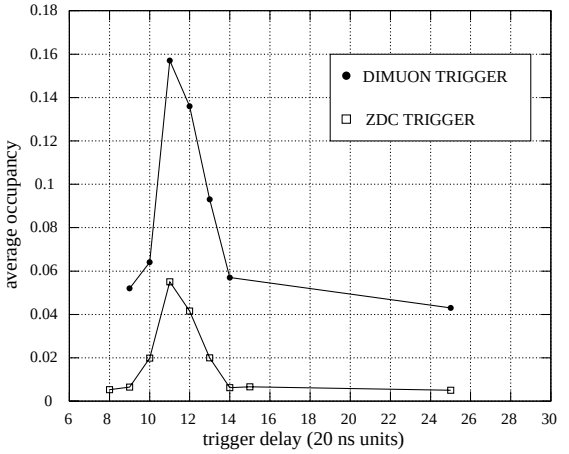

Fig. 7. Average occupancy per strip (BOARD1) vs. trigger delay scan for MD1, sectors 29 and 30 (Pb–Pb run of 1998).

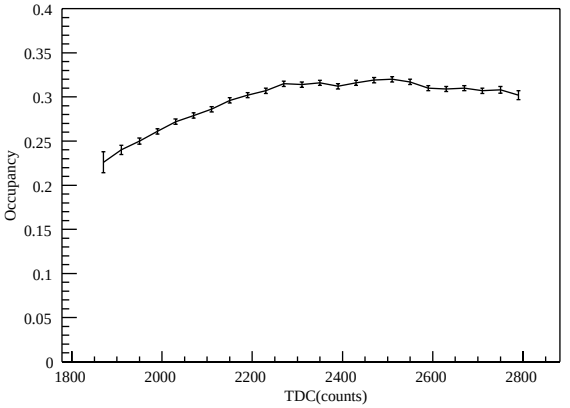

Fig. 8. Average occupancy vs. number of TDC counts (one count $\simeq 25$ ps).

beam intensity (about 10^6 Pb/s) with minimum bias (ZDC) trigger, and for high beam intensity (about 10^7 Pb/s) with dimuon trigger.

The peak occupancy (about 5.5%) with low intensity beam and ZDC trigger corresponds essentially to non-interacting Pb ions giving δ-rays multiplicity plus a small fraction of Pb–Pb interactions. This is almost exactly the same occupancy which is obtained off-peak (for a delay of 25 clock periods) at high intensity with the dimuon trigger. This is expected, since for the high probability of beam pileup at high beam intensity the measured off-peak occupancy becomes similar to the one obtained with minimum bias (ZDC) trigger. The peak occupancy for dimuon trigger is of course higher (about 16%), since it corresponds to the inelastic Pb–Pb interactions, and is found for the same delay value as for the ZDC trigger.

Since the actual sampling instant of the FABRIC discriminator output must be in phase with the free-running CDP clock, the sampling efficiency may depend on the time difference between sampling and trigger (the latter is strictly related to particles crossing the detector), which is recorded by a TDC, as explained in Section 3. Usually there is a wide efficiency plateau, as shown in Fig. 8, and only a small TDC-based offline correction is necessary when evaluating the total multiplicity.

5.2. The discriminator threshold voltage

In order to set the correct discriminator threshold of the analog chip and to measure the signal-to-noise ratio (S/N) of our system, a few threshold scans with the SPS proton beam impinging directly on the detector were made in 1997. Fig. 9 shows the unnormalized integral occupancy curve and its derivative. To be precise, the differential curve should be fitted as a convolution of a Landau curve, reflecting the energy deposition fluctuation, and a Gauss curve reflecting the noise level. In order to estimate the MIP peak position a simple Gaussian fit is performed only in the region around the peak of the differential curve.

From these curves we estimate the MIP peak to be at about 470 mV. The Gaussian noise evaluation from a separate study with pulser gave $\sigma_{\text{noise}} \sim 30$ mV, and this would result in the S/N ratio of about 15. In fact during standard Pb–Pb runs operation of the whole system we observed higher rate of noise counts than expected from the measured σ_{noise}. This could be attributed to pick-up from the digital part of front-end electronics. One should remember that a binary system working at strip occupancy of about 10–30% has a very high rate of switching between high and low voltage states, which could give rise to some non-Gaussian noise component observed during detector operation on the beam. Taking into account

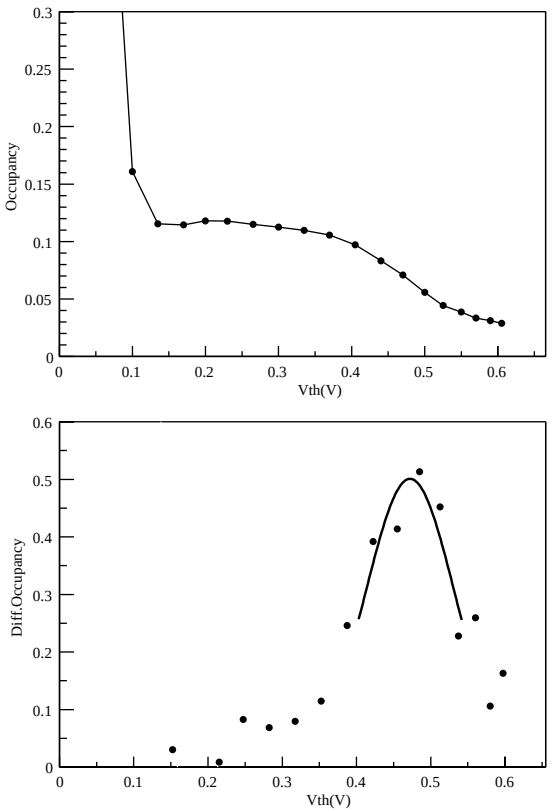

Fig. 9. Occupancy per strip versus threshold voltage with proton beam, after the 1996 ion run (top: integral curve, bottom: differential curve with Gaussian fit).

the system performance in standard conditions we fixed the FABRIC threshold at the relatively high value of about 200 mV. This value was adjusted several times during different years of operation separately for MD1 and MD2 detector planes. Threshold scans taken with secondary particles produced in Pb–Pb interactions were recorded from time to time for this purpose and in particular for BOARD2 DC-coupled detectors, where the increase of the leakage current with time induces a shift of the FABRIC working point.

5.3. The geometrical alignment

The two MD planes are placed orthogonally to the beam line (Z-axis), with X- and Y-axis on the plane of the detector. The pseudorapidity and azimuthal coverage of each strip was determined in the following way:

- the position of each detector with respect to geometrical references in the supporting stesalite disc was measured with an accuracy of about 50 μm (strips 1 and 128 were measured on BOARD1, strips 158–160 on BOARD2);
- these geometrical data, together with the beam width and the positions of targets and of the supporting discs of MD1 and MD2, were used in a simple geometrical Monte-Carlo program to compute, for each target, the distribution of strips on MD2 corresponding to a given strip on MD1 for each sector. This is done under the assumption that the corresponding strips are defined from the position of MD1 and MD2 hits by a particle originating from the chosen target;
- the MD1–MD2 strip correspondences were obtained also from real data where, for events with a particular MD1 strip being hit, the peak position and width in the MD2 occupancy map was found;
- the correspondences obtained from the geometrical Monte-Carlo were compared with the ones extracted from real data;
- the beam offsets in X and Y adopted in the Monte-Carlo were tuned until a good agreement with real data was obtained: the beam offsets found in this way were about 1 mm in Y and 0 mm in X, with a precision of about 0.2 mm.

In Fig. 10 the correspondence between strips of MD1 and MD2 for data (points) and Monte-Carlo (crosses) is shown for sector 9, targets 3, 4 and 5. The curves for different targets (separated by 25 mm) are parallel as expected; the separation between these curves makes it possible to use the MD as a target identification tool.

6. Multiplicity Detector operation and radiation effects

The MD was used in a preliminary configuration (BOARD1s only, 25 MHz sampling frequency) during the 1995 Pb–Pb run and was

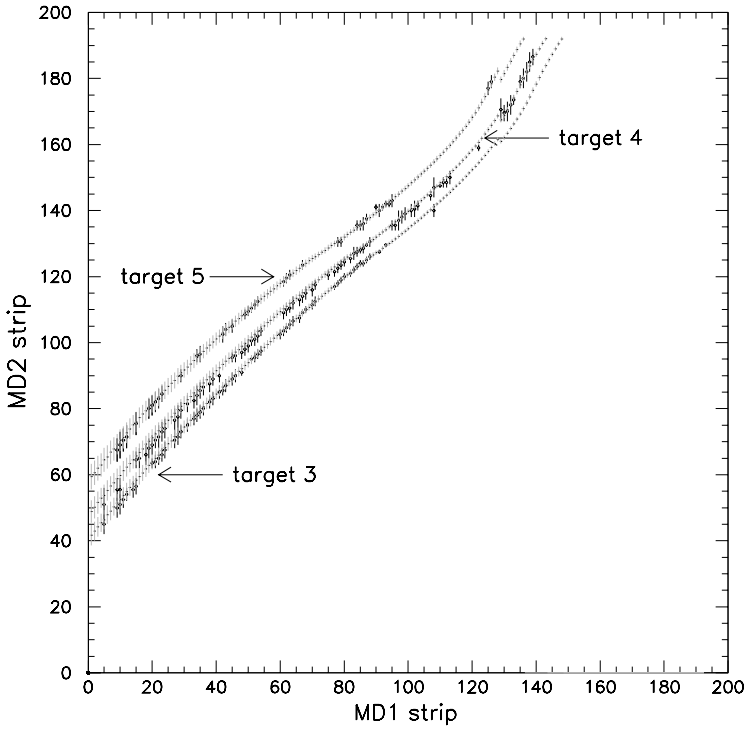

Fig. 10. The MD1–MD2 strip correspondence of sector 9, target 3, 4 and 5.

fully available at 50 MHz sampling frequency for the Pb–Pb runs of 1996, 1998, 1999 and 2000. The BOARD1 with AC-coupled detectors showed a stable operation and a good efficiency except for some older detectors which suffered for the underdepletion in the first (innermost) strips due to heavy radiation damage, as discussed below. The impact of this problem was reduced by replacing several detectors between the 1996 and 1998 runs. On the other hand, operation of the BOARD2 with DC-coupled detectors together with the FABRICs was rather difficult due to the leakage current flowing directly into the FABRICS's input transistor and increasing with radiation. The increase of leakage current caused variations in the working point of the preamplifiers, so that a compromise was made when choosing it, and not all BOARD2s reached a good efficiency.

A specific problem which was observed during heavy ion runs was the presence of many strip clusters, i.e. groups of two or more contiguous detector strips firing at the same time. We observed an increase of the average cluster size in high multiplicity conditions, while for example with low intensity direct proton beam (one track per event) the observed cluster size was compatible with the expectations from charge sharing between adjacent strips due to the track angle plus charge diffusion in a limited region between the strips.

In order to evaluate the true particle occupancy per strip in a small group of $\simeq 10$ adjacent strips, instead of counting of the number of hit strips, the observed cluster size distribution was compared to the one expected from Poisson statistics at given particle occupancy, modified by the introduction of the channel to channel cross-talk probability coefficients. The true occupancy and the coefficients were optimized via an iterative procedure. From this analysis it appears that there is a substantial probability for cross-talk effects in BOARD1 detectors on top of charge diffusion effects and inclined tracks. The most relevant cross-talk mechanisms turned out to be the following: (a) one particle giving 2 or 3 firing strips (respective probabilities ~ 0.2, ~ 0.07), and

(b) turning on of 1 or 2 empty strips located between two firing strips (respective probabilities ~ 0.6, ~ 0.2). These probability coefficients include both physical (track angle and charge diffusion) and instrumental effects. The reason for instrumental effects may be the superposition of non-Gaussian noise due to digital pick-up, cross-talk in the connections between strips and the front-end chip and a shift of the effective discriminator threshold under high counting rate conditions.

The ratio between apparent and true detector occupancy ranges from ~ 1 for peripheral (low multiplicity) events to ~ 1.8 for central (high multiplicity) events.

6.1. Radiation effects

Detailed results about radiation effects on the multiplicity detector were shown in Refs. [11–13]. The main effects observed during the periods of detector operation were the increase of leakage current and the variation of the full depletion voltage. The leakage current was continuously measured during the data taking by our dedicated slow control system. A plot of the leakage currents (recorded on file every 2 h) from 1996 to 2000 is shown in Fig. 11 for two typical BOARD1 detectors, namely one already used in 1995 and another used for the first time in 1996. It can be observed a steady increase of leakage current with time due to detector irradiation. The discontinuities are due to periods without beam, during which the temperature of the detector decreased because the front-end chips were turned off, to switching off and on the detector cooling system and to changes of the detectors bias voltage. The reverse annealing, i.e. the long-term increase of the effective doping concentration, was limited by keeping the MD at -24°C temperature during the months in between data taking periods.

Due to radiation-induced change of the doping concentration, the full depletion voltage for the

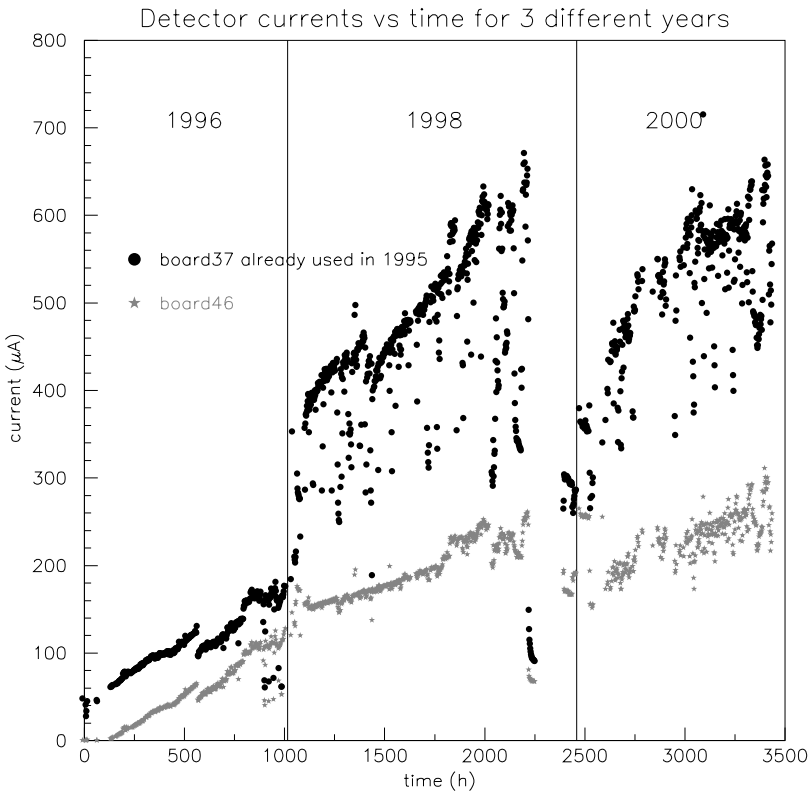

Fig. 11. Leakage current (μA) as a function of beam time (hours) for two BOARD1s during Pb–Pb runs of 1996, 1998 and 2000.

inner part of BOARD1 detectors (which was the most heavily irradiated) decreased at first and then increased again after type inversion. The depletion voltage was monitored periodically during data taking by means of High Voltage (HV) scans, where the average occupancy vs. detector bias voltage was measured for groups of nearby strips. An example of such a HV scan is shown in Fig. 12. In the upper plot the strip occupancy versus bias voltage is shown for a typical new detector at the beginning of the 1998 run. All strips have the same depletion voltage of about 30 V. The absolute strip occupancy differs between inner and outer strips because it reflects the physical particle occupancy and so it is not relevant for the depletion voltage estimation. In the lower plot the result of a HV scan performed during year 2000 run is presented. The innermost strips which received the highest particle fluence are far beyond type inversion, what is reflected by the high value of the depletion voltage which may be estimated from the plot. For more external strips the depletion voltage becomes lower and lower reaching values close to type inversion point for the outermost strips.

The depletion voltage was cross-checked for some detectors by means of C–V measurements in the laboratory and was found to be in agreement with the one obtained with the HV scan [12,13].

Table 2 shows a summary of the HV settings for individual detectors of the two planes MD1 and MD2, separately for BOARD1 and BOARD2, during the data taking period 1995–2000. The standard HV value for BOARD1s was gradually increased between the beginning and the end of each year's data taking, as indicated in the table. After 1996, the MD was completely disassembled and many detectors were replaced. From the last column of the table we see that some BOARD1 detectors were set at 200 V: this means that the full depletion voltage of the inner strips for them became with time higher than our power supply limit of 200 V. These BOARD1 detectors were then set at 200 V for the remaining data taking time, to obtain full depletion for as many strips as possible. BOARD2 detectors were always fully depleted.

For the front-end electronics, due to its position further away from the beam axis, the received

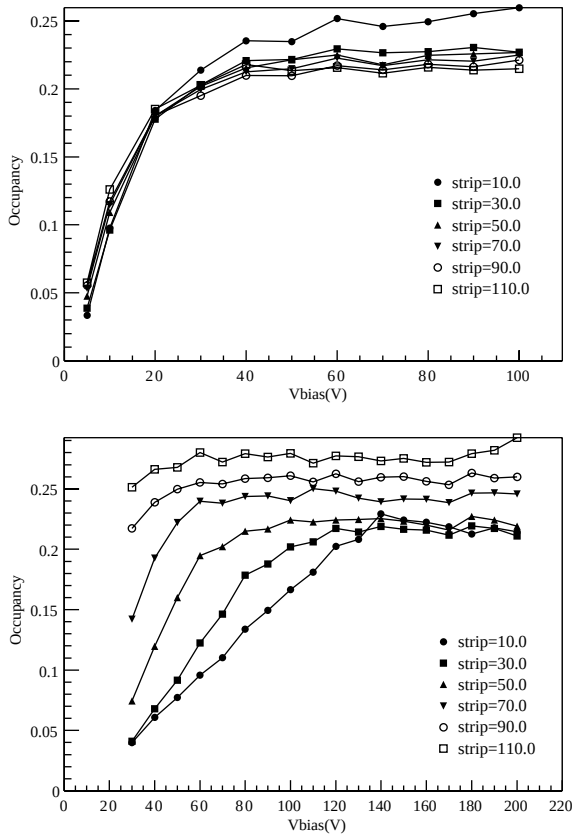

Fig. 12. Occupancy vs. high voltage for a group of strips of MD1 sector, in two successive periods of data taking.

radiation levels were much smaller than for the innermost strips of the detectors. We estimate the integrated fluence to be below 10^{12} equivalent 1 MeV neutrons/cm^2 and the total dose to be about 200 krad. For digital chips (CDPs) produced in radiation resistant technology no radiation effects were observed. Radiation-induced latchup events were observed [14] for a few prototype CDPs which were manufactured using a non-radiation resistant process. Also for analog chips (FABRICs) we did not observe any noticeable change of performance. But one should remember that for our binary readout architecture a small performance degradation may be undetectable without accurate measurements, which could give an estimation of a possible decrease of FABRICs transistor gain (beta) and increase of noise.

Table 2
HV settings for the two planes, MD1 and MD2, during the data taking from 1995 until 2000

Data taking year	MD plane	Standard HV (V)		Fully depleted detectors	Underdepleted detectors (HV set at 200 V)
		Board1 Begin → end	Board2	Board1	Board1
1995–1996	MD1	60 → 110	80	18	—
	MD2	60 → 110	80	18	—
1998	MD1	90 → 130	90	11	7
	MD2	90 → 110	90	13	5
1999	MD1	130 → 150	90	9	9
	MD2	110 → 130	90	14	4
2000	MD1	170	140	9	9
	MD2	160	140	14	4

7. Multiplicity Detector results

7.1. Target identification

An important result from the MD is the identification of interactions coming from the target, which must be separated from those due to Pb–air interactions or upstream/downstream interactions. The identification is based on the comparison of estimators for different target positions, using the MD1–MD2 correspondences shown previously. The estimators are defined as the ratio of found MD1–MD2 strip correspondences to possible correspondences, under different hypotheses on the interaction position (namely target(s), nearby surrounding air and target box windows). A scatter plot of the largest (winning) estimator vs. the forward energy in the 1998 data taking is shown in Fig. 13. The estimator reaches higher values for central interactions because the occupancy of both MD1 and MD2 becomes higher and the probability of random correspondences increases. The straight line represents the cut adopted to separate the interacting Pb ions from the non-interacting ones. The peak of non-interacting beam is at 33,000 GeV forward energy, while the cut provides an event sample with sufficiently low contamination up to about 25,000 GeV.

The target identification method based on MD offered a higher efficiency (and a better separation from Pb–air interactions) for peripheral Pb–Pb interactions with respect to the method based on quartz blades, allowing the analysis of charmonium suppression to be extended down to lower centralities [15].

7.2. Centrality estimation

The MD provided centrality estimation via global measurements of charged multiplicity, including both the region of the maximum particle density per pseudorapidity unit and the region of the dimuon spectrometer acceptance. As an example, the correlation between multiplicity in the spectrometer coverage (MUL1) and E_T and the correlation between the two MD planes are shown in Fig. 14.

7.3. Charged multiplicity

The MD provided also detailed pseudorapidity distributions with a good angular coverage, as a function of centrality, for two beam energies [16]. Two analyses were performed using two independent centrality-related observables: the energy of the projectile spectator nucleons measured by the ZDC and the neutral transverse energy measured by the EMC. In both cases, the centrality selection was made using observables which are independent of the multiplicity detector itself, in order to avoid autocorrelations. Special runs taken with the minimum bias trigger at low beam intensity (about $\frac{1}{10}$ of the standard intensity used by the experiment) were used: the first data sample was taken in 1998 at 158 GeV per nucleon incident energy, the

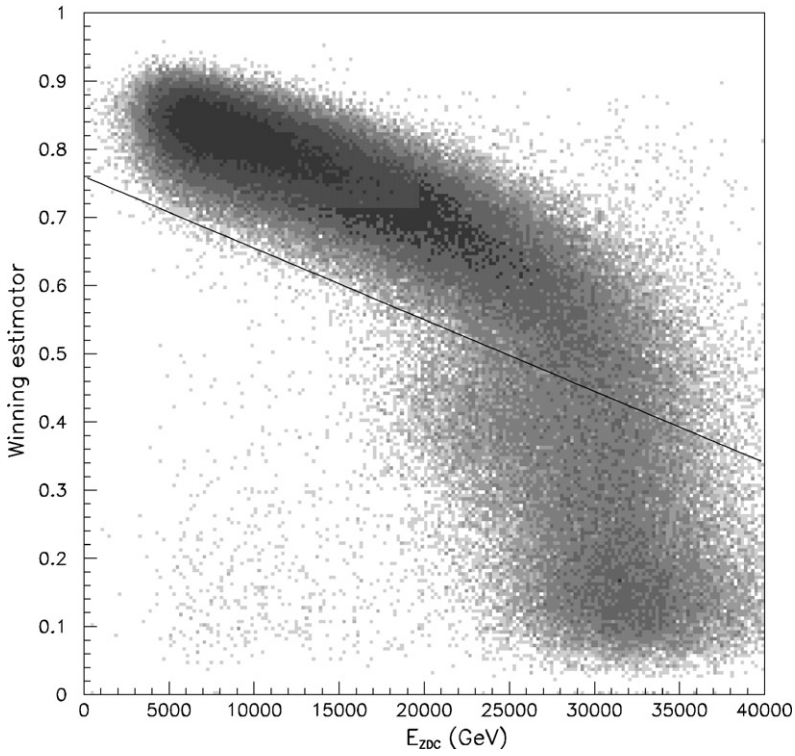

Fig. 13. Winning target estimator vs. E_{ZDC} (GeV).

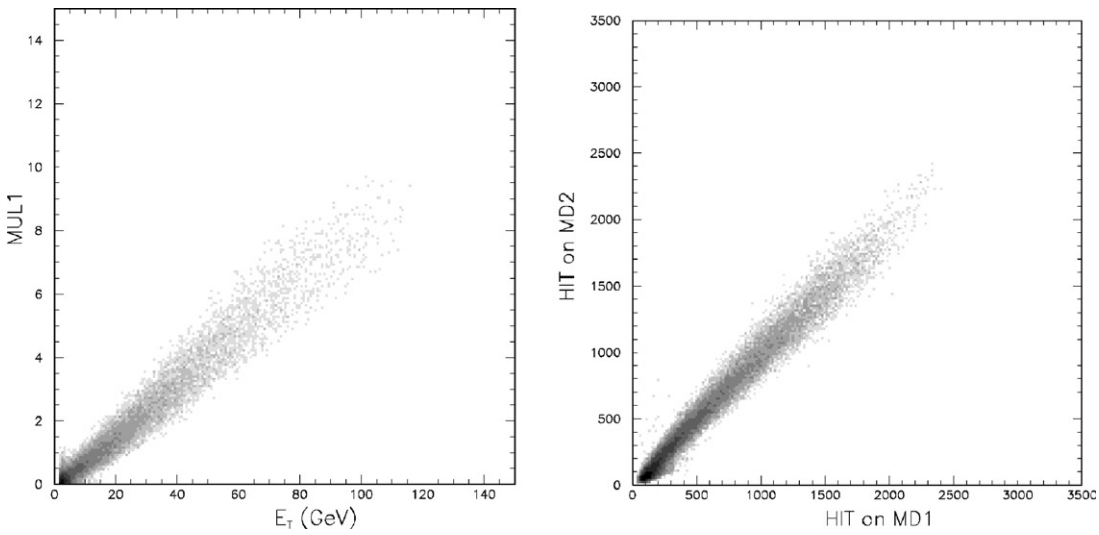

Fig. 14. Correlation between: charged multiplicity per sector and E_T (left), total MD1 and MD2 multiplicity (right).

second in 1999 at 40 GeV/nucleon energy. The charged particle pseudorapidity distributions ($\mathrm{d}N_{\mathrm{ch}}/d\eta$) in Pb–Pb collisions were measured in 6 centrality classes defined in terms of fractions (between 0% and 35%) of the total inelastic cross-section. For more details, see Ref. [16].

8. Conclusions

We have designed, built and operated a high-granularity silicon strip detector for charged multiplicity measurement in the challenging environment of the NA50 experiment. Very severe spatial and timing constraints (driven by the need of minimizing decays of pions and kaons and maximizing the luminosity) have been satisfied with a design based on two VLSI fast front-end chips featuring 50 MHz clock frequency. The radiation tolerance of the two front-end chips has been demonstrated. The silicon detectors, located in a very high radiation environment, have worked efficiently even beyond the type inversion point of n-type silicon. The MD has provided centrality measurement and subtarget identification in Pb–Pb collisions for the NA50 data taking between years 1995 and 2000. The charged particle pseudorapidity distributions as a function of centrality have also been obtained.

Acknowledgements

We are grateful to the members of the NA50 collaboration who provided a stimulating and friendly framework during the construction and operation of the detector. In particular we thank C. Baglin and V. Capony for their help with the readout system and M. Forlen for his cooperation in the development of the front-end VME modules.

We acknowledge useful discussions with P. Burger during the development of the detector design. We are grateful to the DEM group of the EST Division at CERN, in particular to D. Berthet, A. Gandi, L. Mastrostefano, C. Millerin, A. Monfort and M. Sanchez for help in developing the multilayer printed circuit boards and the kapton cables. We thank O. Runolfsson for making his bonding and mechanical measuring equipment available to us, and for useful discussions.

We are deeply indebted to E. Bollito, who did personally most of the bonding work and developed techniques to reuse existing boards by replacing the radiation damaged detector on them. We thank B. Pini for help in repairing mechanically damaged detectors. We are grateful to L. Simonetti and S. Brasolin for designing the mechanical support and to G. Alfarone, F. Daudo, M. Mucchi for help during its construction. We thank P. Barberis, F. Benotto, E. Filoni and F. Rotondo for support in setting up and maintaining the front-end electronics.

Financial support from the Istituto Nazionale di Fisica Nucleare of Italy is acknowledged. This work was supported in part by the Polish State Committee for Scientific Research, Project No. 2P03B03319.

References

[1] M.C. Abreu, et al., Study of muon pairs and vector mesons produced in high energy Pb–Pb interactions, Proposal CERN/SPSLC 91-05, SPSLC/P265, October 1991.
[2] T. Matsui, H. Satz, Phys. Lett. B 178 (1986) 416.
[3] R. Arnaldi, et al., Nucl. Instr. and Meth. A 411 (1998) 1.
[4] F. Bellaiche, et al., Nucl. Instr. and Meth. A 398 (1997) 180.
[5] ATLAS Inner Tracker Technical Design Report, Vol. 2, CERN/LHCC/97-17, p. 394.
[6] W. Dabrowski, et al., Nucl. Instr. and Meth. A 350 (1994) 548.
[7] P. Barberis, et al., Nucl. Phys. B 32 (1993) 540.
[8] J. DeWitt, IEEE Nuclear Science Symposium, San Francisco, October–November 1993.
[9] V. Capony, Ph.D. Thesis, Université de Savoie, 1996.
[10] A. Gramaglia, Thesis, Università di Torino, 1998.
[11] B. Alessandro, et al., Nucl. Instr. and Meth. A 409 (1998) 167.
[12] B. Alessandro, et al., Nucl. Instr. and Meth. A 419 (1998) 556.
[13] B. Alessandro, et al., Nucl. Instr. and Meth. A 432 (1999) 342.
[14] B. Alessandro, et al., Nucl. Instr. and Meth. A 476 (2002) 758.
[15] F. Prino, Ph.D. Thesis, Università di Torino, 2001.
[16] M.C. Abreu, et al., Phys. Lett. B 530 (2002) 33.